

The diffusion of carbon atoms inside carbon nanotubes

Yanjie Gan,¹ J. Kotakoski,^{2,3} A. V. Krashennnikov,^{2,4} K. Nordlund,² and F. Banhart,^{1,5}

¹Institut für Physikalische Chemie, Universität Mainz, D-55099 Mainz, Germany

²Accelerator Laboratory, P.O. Box 43, FIN-00014 University of Helsinki, Finland

³Institut für Materialwissenschaft, Technische Universität Darmstadt, Petersenstraße 23, D-64287 Darmstadt, Germany

⁴Laboratory of Physics, Helsinki University of Technology, P.O.Box 1100, Helsinki 02015, Finland

⁵Institut de Physique et Chimie des Matériaux IPCMS-GSI, UMR 7504, 23 rue du Loess, 67034 Strasbourg, France

Abstract.

We combine electron irradiation experiments in the transmission electron microscope with kinetic Monte Carlo simulations to determine the mobility of interstitial carbon atoms in single-walled carbon nanotubes. We measure the irradiation dose necessary to cut nanotubes repeatedly with a focused electron beam as a function of separation between the cuts and at different temperatures. As the cutting speed is related to the migration of displaced carbon atoms trapped inside the tube and to their recombination with vacancies, we obtain information about the mobility of the trapped atoms and estimate their migration barrier to be about 0.25 eV. This is an experimental confirmation of the remarkably high mobility of interstitial atoms inside carbon nanotubes, which shows that nanotubes have potential applications as pipelines for the transport of carbon atoms.

1. Introduction

The application of single-walled carbon nanotubes (SWNTs) in many fields of nanotechnology relies on our ability to tailor locally the structure and properties of the tubes. In addition to chemical methods, this can be done by spatially localized irradiation with energetic particles combined with high-temperature annealing. Recent experiments demonstrate that electron or ion beams can serve as tools to change the morphology of nanotubes with nearly atomic precision [1, 2, 3, 4, 5]. Moreover, in many cases irradiation leads to structural self-organization or self-assembly in carbon nanostructures (see Ref. [6] for an overview). All these phenomena are due to a delicate balance between defect creation and annealing. Therefore, detailed knowledge of migration and annihilation of defects in nano-structured carbon materials is indispensable.

Point defects in nanotubes are vacancies (missing atoms in the atomic network) and interstitials which, for tubular materials, can be thought of as carbon atoms attached to the nanotube inner or outer surface. While a lot of theoretical work on diffusion of point defects has already been done [7, 8, 9, 10, 11], there is, to our knowledge, no quantitative experimental information on the mobility of such defects. Although recent in-situ experiments in the transmission electron microscope (TEM) made it possible to monitor defect evolution at room [4, 12] and elevated [13] temperatures, the low visibility of point defects and the limited time resolution did not allow for a precise measurement of defect migration barriers. The data on mobility of defects in planar graphite can hardly be relevant to nanotubes due to the curvature of the graphitic network in nanotubes, which breaks the trigonal symmetry of the graphene sheet. Moreover, recent theoretical results [14, 15] contradict the old experimental data on migration energies of point defects in graphite [16].

In the present study we obtain quantitative experimental information on the mobility of carbon interstitials in SWNTs by cutting bundles of SWNTs with a strongly focused electron beam at various temperatures. As the cutting speed is related to the defect annealing rate, such a setup makes it possible to measure the migration barrier for carbon atoms trapped inside SWNTs. To validate the interpretation of the results and to get a complete picture of defect migration, we also carry out kinetic Monte Carlo simulations.

2. Experimental

2.1. Experimental setup and technical details

As we have reported earlier [17], when a SWNT is cut by an electron beam, a certain number of vacancies must be created until cutting is achieved (the gap is actually an agglomerate of vacancies). Once a SWNT has been cut, the open ends close by fullerene caps as shown in Fig. 1(a). Such a cap closes the tube for interstitial atoms created by the electron beam, and migrating inside the nanotube. When a second cut is being

made, the interstitials are reflected at the closed end and have a higher probability to migrate back to the second cut from where they stem, thus lowering the cutting speed due to their annihilation with vacancies in the gap. The situation is schematically shown in Figs. 1(b) and (c). In this work we cut SWNTs at different separations L between the closed end (first cut) and the second cut and measure the electron dose necessary for making the second cut as a function of L .

In our experiments, commercially available bundles of SWNTs were heated to temperatures in the range 400–900°C in the heating stage of a TEM. Imaging and electron irradiation was undertaken in a TEM with a field emission gun (FEI Tecnai F-30) at an electron energy of 300 keV. Cutting of the SWNT bundles was carried out at typical beam current densities of 2000 - 4000 A/cm² on the nanotubes by focusing the electron beam onto a spot of 4-5 nm in diameter (FWHM of the Gaussian beam profile). Although irradiation in a spot does not offer good imaging conditions, the tube under the beam can still be seen while the cut is being made.

2.2. Measuring cutting speed at different separations between the cuts

At first, a SWNT bundle was cut somewhere far away from the ends. The measurement of the electron dose necessary for cutting was carried out by moving the electron beam across the SWNT bundle with such a speed that cutting was just achieved (a lower speed would waste electrons because the gap has already been made; a larger speed would result in damage but not complete cutting). Then, at a certain distance from the first cut, the bundle was cut the second time and the cutting speed was measured again in the same way. The procedure was carried out for various distances between the cuts at 400, 600, and 900°C. For each measurement of the electron dose, a new SWNT bundle was chosen, i.e., a new first cut was made and then the dose for the second cut at a certain distance from the first cut was measured. The cutting of a pristine SWNT (first cut) needed a typical electron dose of approximately 10⁹ electrons/nm², independent of temperature, and took somewhat less than 5 seconds under the present conditions.

Previous studies [10, 8] indicated that the diffusivity of C atoms is higher on the inner surface of the nanotube than for those on the outer surface. Here we denote C atoms inside SWNTs as interstitials, and atoms adsorbed on the outer surface as adatoms. The interstitial can also penetrate the nanotube shell by the exchange mechanism, but the barrier for such a process is at least one order of magnitude higher than for the diffusion along the axis [18]. Thus the diffusion of interstitials should be the factor that governs the cutting speed.

Several complications had to be taken into account. We deal with nanotube bundles, not with individual SWNTs, so that the mobility of atoms on the outer surface could possibly be influenced by adjacent tubes. Nevertheless, one can expect that the presence of nearby tubes and reduction of open space will make the migration of C atoms inside inter-tube channels even slower than for free-standing SWNTs. Besides, we found that the cutting speed for the first cut v_1 is influenced by the structural perfection

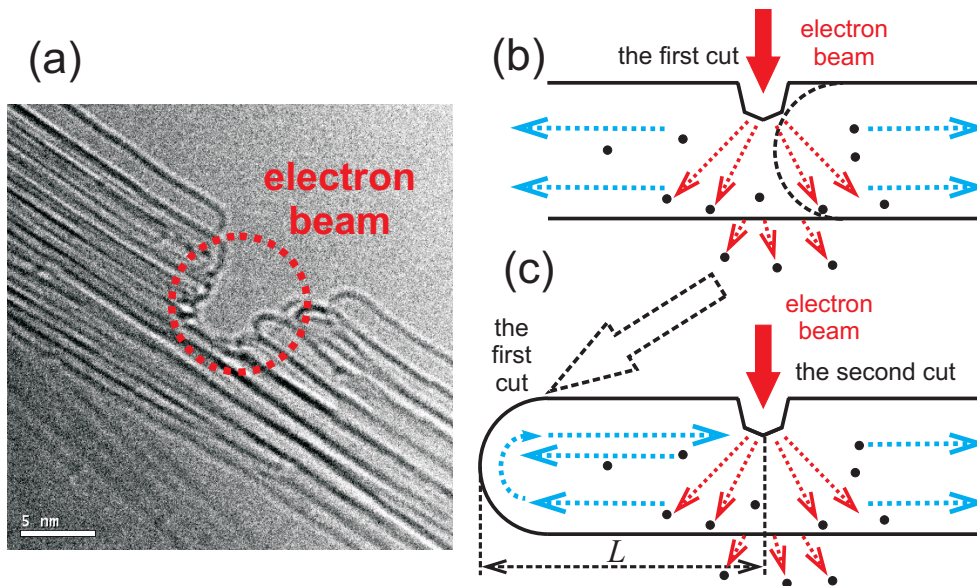


Figure 1. Nanotubes cut by the electron beam. (a) TEM picture of a nanotube bundle partially cut by the beam. It is evident that tubes develop caps at the cuts. (b) Schematic representation of a nanotube within the bundle when the first cut is being made. The interstitials created by the beam migrate away from the cut into both directions and disappear. (c) During the development of the second cut, the interstitials have a higher probability to arrive at the cut due to 'reflection' from the cap and to annihilate with vacancies thus slowing down the cutting speed.

of the tubes and varied from bundle to bundle. By measuring v_1 on many independent SWNT bundles in the same specimen, we found from the scatter of the values that the experimental error, including uncertainties in the measurement of the cutting speed and possible variations of the necessary dose to cut tubes of different chiralities, is about 20%. At large separations between the cuts the cutting speed for the second cut v_2 saturated towards v_1 within the experimental error, as expected. To account for minor deviations between v_1 and $v_2(L \rightarrow \infty)$ (less than 5% at 600 and 900°C and about 14% at 400°C), we assumed that $v_1 = v_2(L \rightarrow \infty)$ and used this value below to calculate relative cutting speed v_2/v_1 .

In Fig. 2 v_2/v_1 is presented as a function of separation L between the first and the second cut. It is evident that the cutting speed is affected by the presence of the first cut at small separations, but this effect vanishes with increasing L . It is also clearly seen that for a certain L the ratio decreases with temperature. As mentioned above, at 400°C $v_2(L \rightarrow \infty)$ saturates towards a value which is 14% less than v_1 . The origin of such a behavior is not fully understood. A possible explanation is different annealing of pre-existing defects such as small carbon clusters at different temperatures or the agglomeration of defects created during the first cut.

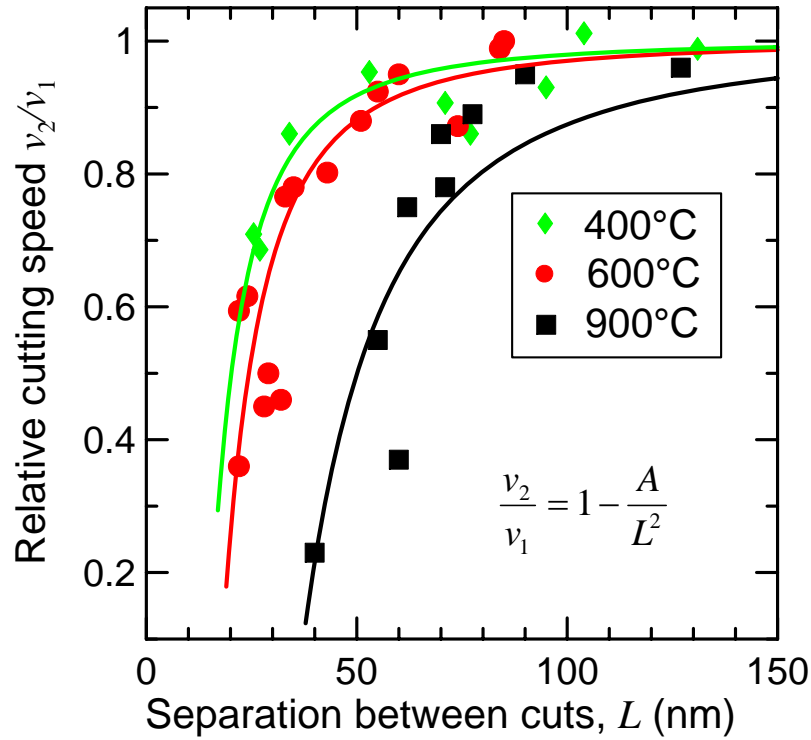


Figure 2. Relative cutting speed v_2/v_1 at various temperatures as a function of separation between the cuts L . Symbols stand for the experimental data, solid lines are fits obtained with Eq. (4). All curves were scaled to $v_1 = v_2(L \rightarrow \infty)$. The error of each measurement is approximately 20%.

3. Discussion

3.1. Determination of the migration barrier within the framework of a simple analytical model

If a drop in the cutting speed at small separations originates from a different distribution of interstitials in nanotubes, which is affected by temperature and the presence of the cap at the first cut, we can assume that the cutting speed is

$$v_2 = v_1 - \Delta v \quad (1)$$

where Δv is a drop in the cutting speed due to the recombination of vacancies at the second cut with the interstitials "reflected" back from the first cut. Δv is proportional to the number n of the interstitials which recombined with vacancies. The higher n , the slower is the cutting process. One can further assume that $n \sim \tau^{-1}$, where τ is the time required for the interstitial to travel to the end of the tube and back.

It is known that in a quasi-one-dimensional system [19],

$$\tau \sim L^2/D, \quad (2)$$

where D is the diffusion coefficient for the created defect,

$$D = D_0 \exp[-E_m/kT], \quad (3)$$

D_0 is a constant, E_m is the migration barrier, k Boltzmann's constant.

By combining Eqs. (1-3), one can express the relative cutting speed v_2/v_1 in terms of E_m and L :

$$v_2/v_1 = 1 - A(T)/L^2, \quad (4)$$

$$A(T) = A_0 \exp[-E_m/kT]. \quad (5)$$

The migration barrier E_m can now be deduced from the experimental data presented in Fig. 2 by fitting coefficients A using Eqs. (4,5) at different temperatures. The best fit gave $E_m = 0.25 \pm 0.05$ eV. The lower and the upper bounds on E_m can also be determined by taking into account only two lower (400°C and 600°C) and higher (600°C and 900°C) temperatures, which gave 0.1 and 0.4 eV respectively. Thus, based on the experimental results, one can conclude that the migration energy (along the tube axis) of single interstitials inside the open hollow of the nanotubes is indeed quite small, in the range of 0.2 – 0.3 eV, corroborating the predicted theoretical results [10, 8].

3.2. Kinetic Monte Carlo simulations

As a nanotube is not a real one-dimensional system and thus various diffusion paths for point defects are possible, we used our recently developed kinetic Monte Carlo (kMC) code [18] to gain insight to the atomic scale processes occurring during the electron irradiation. The code allows simulating the migration of point defects on a SWNT on the macroscopic time scale (up to several minutes), their annihilation and clustering, and thus the response of the SWNT to electron irradiation. The implemented defects include single vacancies, adatoms and interstitials. The migration energies and annihilation characteristics were obtained from density functional theory-based calculations [10, 11, 8].

To mimic the experimental conditions, we simulated irradiation of an armchair (10,10) nanotube with a length of 2 μm and diameter of 1.3 nm, close in size to the nanotubes used in the experiments. The closure of the structure due the first cut was modeled as a hard wall reflecting all incoming defects. Based on the experimental conditions and displacement cross-section estimates [20, 21], the beam was assumed to produce 2.5 displacements/atom sec with a Gaussian probability distribution around the center of the beam.

The results of our simulations at $T = 400^\circ\text{C}$, 500°C , and 600°C and for L in the range of 10-90 nm are shown in Fig. 3. Each point is an average over 200 independent runs to obtain reasonable statistics. We could not run simulations at temperatures higher than 600°C due to computational limitations, since the simulation time needed to cut a SWNT increases exponentially with temperature within our computational model. This resulted in a high scatter in the kMC results at 600°C so that we did not fit the data.

As a test, the fit of the kMC results by Eqs. (4,5) gave a value of $E_m \sim 0.32$ eV. As the migration energy of interstitials inside the open hollow of a (10,10) nanotube

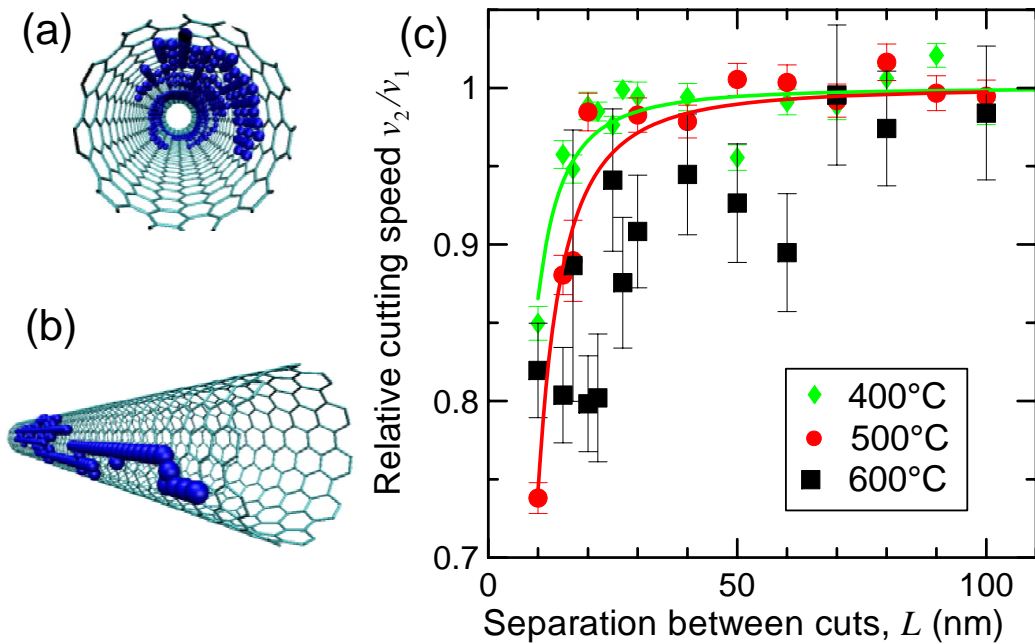


Figure 3. Results of kMC simulations. (a) Trajectory of an interstitial inside a (10,10) nanotube at $T = 500^\circ\text{C}$ during 30 nanoseconds. (b) Trajectory of an adatom at $T = 500^\circ\text{C}$ during 1 millisecond. Note the difference in the time scale. (c) Relative velocity for the second cut as obtained by the kMC simulations as a function of the separation between the cuts. Solid lines show the theoretical curves obtained through Eq. (5) at different temperatures

was set 0.35 eV [8] in our kMC simulations, this result confirms that the drop in cutting speed can be understood within the simple theoretical model described by Eq. (2). The detailed analysis of the trajectories showed that interstitials tend to spiral inside the tube, while the trajectories of adatoms are closer to straight lines due to curvature effects [8], as shown in Figs. 3 (a,b). Although adatoms (with migration barrier of about 0.7 eV) also contribute to annealing at temperatures over 500°C , the different motion of the migrating species favors annihilation of interstitials with vacancies, as the probability for an interstitial to 'meet' a vacancy is higher.

We stress that we did not deliberately fit any parameters in our kMC code to reproduce the experimental results. It is known that carbon nanotubes shrink under irradiation [10], while kMC simulations are carried out on a fixed lattice. There may also be a barrier for recombination between interstitials and vacancies due to the formation of new bonds at pentagons [11], especially in double vacancies. Besides this, in experiments interstitials can be incorporated into the lattice at the first cut and annihilate with pre-existing defects due to restructuring of the carbon network, which is beyond the kMC model. Thus, one cannot expect more than qualitative agreement between the experimental and simulation data.

Assuming that the migration length of interstitials during the time between two

electron impacts is comparable to the separation between the cuts, and using the migration barrier of around 0.3 eV, one can estimate the prefactor D_0 in Eq. (3). The values proved to be smaller by approximately one order of magnitude than the conventional value of the prefactor given by $a^2\nu_0$, where a is the C atom jump length and ν_0 is jump frequency, $\nu_0 = 4 \times 10^{12} \text{ sec}^{-1}$ [16]. Smaller values can be expected, as the interstitials tend to spiral inside nanotubes, so that their diffusion is correlated. Nevertheless, the diffusivity of interstitials in carbon nanotubes (along the tube axis) can be described through Eq. (3), if a correlation factor of about 0.1 is introduced, so that $D_0 \sim 0.1a^2\nu_0$. This is the average value for SWNTs: the diffusivity of interstitials in a particular tube should depend on its chirality.

4. Conclusions

To conclude, by combining electron irradiation experiments with kinetic Monte Carlo simulations we determined the migration barrier of carbon interstitials inside the inner hollow of single-walled carbon nanotubes, which proved to be about 0.25 eV. This is an experimental confirmation of a high mobility of interstitial atoms inside carbon nanotubes, which corroborates the theoretical model of interstitial diffusivity. Hence, we can confirm that single-wall carbon nanotubes act as efficient pipelines for the transport of carbon atoms. This is of importance in all applications where point defects are created in the tubes [1, 2, 3, 4, 5, 10, 17] and thermal annealing [12, 22] is used to heal the defect structures.

5. Acknowledgement

We thank the DAAD and ETC for an exchange grant (D/05/51651) and the Academy of Finland for the support through several projects and the Centre of Excellence programme. We are also indebted to the Finnish Center for Scientific Computing for generous grants of computer time.

References

- [1] A. Kis, G. Csányi, J.-P. Salvetat, T.-N. Lee, E. Couteau, A. J. Kulik, W. Benoit, J. Brugger, and L. Főrro. Reinforcement of single-walled carbon nanotube bundles by intertube bridging. *Nature Mater.*, 3:153–157, 2004.
- [2] G. Gómez-Navarro, P. J. De Pablo, J. Gómez-Herrero, B. Biel, F. J. Garcia-Vidal, A. Rubio, and F. Flores. Tuning the conductance of single-walled carbon nanotubes by ion irradiation in the anderson localization regime. *Nature Mater.*, 4:534–539, 2005.
- [3] M. Terrones, H. Terrones, F. Banhart, J.-C. Charlier, and P. M. Ajayan. Coalescence of single-walled carbon nanotubes. *Science*, 288:1226–1229, 2000.
- [4] A. Hashimoto, K. Suenaga, A. Gloter, K. Urita, and S. Iijima. Direct evidence for atomic defects in graphene layers. *Nature*, 430:870–873, 2004.
- [5] W. Mickelson, S. Aloni, W. Q. Han, J. Cumings, and A. Zettl. Packing C60 in Boron Nitride Nanotubes. *Science*, 300(5618):467–469, 2003.

- [6] A. V. Krasheninnikov and F. Banhart. Engineering of nanostructured carbon materials with electron or ion beams. *Nature Mater.*, 6:723–733, 2007.
- [7] Y. H. Lee, S. G. Kim, and D. Tománek. Catalytic growth of single-wall carbon nanotubes: An ab initio study. *Phys. Rev. Lett.*, 78:2393–2396, 1997.
- [8] A. V. Krasheninnikov, K. Nordlund, P. O. Lehtinen, A. S. Foster, A. Ayuela, and R. M. Nieminen. Adsorption and migration of carbon adatoms on carbon nanotubes: Density functional ab initio and tight-binding studies. *Phys. Rev. B*, 69:073402, 2004.
- [9] A. Maiti, C. J. Brabec, and J. Bernholc. Kinetics of metal-catalyzed growth of single-walled carbon nanotubes. *Phys. Rev. B*, 55:R6097, 1997.
- [10] F. Banhart, J. X. Li, and A. V. Krasheninnikov. Carbon nanotubes under electron irradiation: Stability of the tubes and their action as pipes for atom transport. *Phys. Rev. B*, 71:241408(R), 2005.
- [11] A. V. Krasheninnikov, P. O. Lehtinen, A. S. Foster, and R. M. Nieminen. Bending the rules: Contrasting vacancy energetics and migration in graphite and carbon nanotubes. *Chem. Phys. Lett.*, 418:132–136, 2006.
- [12] Kazu Suenaga, Hideaki Wakabayashi, Masanori Koshino, Yuta Sato, Koki Urita, and Sumio Iijima. Imaging active topological defects in carbon nanotubes. *Nature Nanotech.*, 2:358 – 360, 2007.
- [13] K. Urita, K. Suenaga, T. Sugai, H. Shinohara, and S. Iijima. In situ observation of thermal relaxation of interstitial-vacancy pair defects in a graphite gap. *Phys. Rev. Lett.*, 94:155502, 2005.
- [14] L. Li, S. Reich, and J. Robertson. Defect energies of graphite: Density-functional calculations. *Phys. Rev. B*, 72:184109, 2005.
- [15] R.H. Telling, C.P. Ewels, A.A. El-Barbary, and M.I. Heggie. Wigner defects bridge the graphite gap. *Nature Materials*, 2:333 – 337, 2003.
- [16] P. A. Thrower and R. M. Mayer. Point defects and self-diffusion in graphite. *Phys. Stat. Sol. (a)*, 47:11, 1978.
- [17] F. Banhart, J. X. Li, and M. Terrones. Cutting single-walled carbon nanotubes with an electron beam: Evidence for atom migration inside nanotubes. *Small*, 1:953–956, 2005.
- [18] J. Kotakoski, A. V. Krasheninnikov, and K. Nordlund. Kinetic monte carlo simulations of the response of carbon nanotubes to electron irradiation. *J. Comp. Theor. Nanosci*, 4:1153–1159, 2007.
- [19] V. Meunier, J. Kephart, C. Roland, and J. Bernholc. Ab initio investigations of lithium diffusion in carbon nanotube systems. *Phys. Rev. Lett.*, 88:075506, 2002.
- [20] A. V. Krasheninnikov, F. Banhart, J. X. Li, A. S. Foster, and R.M. Nieminen. Stability of carbon nanotubes under electron irradiation: Role of tube diameter and chirality. *Phys. Rev. B*, 72:125428, 2005.
- [21] A. Zobelli, A. Gloter, C. P. Ewels, G. Seifert, and C. Colliex. Electron knock-on cross section of carbon and boron nitride nanotubes. *Phys. Rev. B*, 75:245402, 2007.
- [22] F. Ding, K. Jiao, Y. Lin, and B. I. Yakobson. How evaporating carbon nanotubes retain their perfection. *Nano Letters*, 7:681–684, 2007.